1 **Title**: Granzyme B prevents aberrant IL-17 production and intestinal pathogenicity in $CD4^+$ T cells

2

3 **Authors**: Kristen L. Hoek, PhD [a]; Michael J. Greer, PhD [b*]; Kathleen G. McClanahan,[a*] Ali Nazmi
4 [a], PhD; M. Blanca Piazuelo, MD[c,e]; Kshipra Singh, PhD[c,e]; Keith T. Wilson, MD[a,c,e,f,g]; and
5 Danyvid Olivares-Villagómez, PhD[a,e,g,h].
6 *These two authors contributed equally to this report

7

8 **Affiliations**: [a]Department of Pathology, Microbiology and Immunology, Vanderbilt University
9 Medical Center, A5301 Medical Center North, Nashville, Tennessee 37232, USA; [b]Department of
10 Biomedical Informatics, Vanderbilt University, Nashville, Tennessee, 37232, USA; [c]Division of
11 Gastroenterology, Hepatology and Nutrition, Department of Medicine, Vanderbilt University
12 Medical Center, Nashville, Tennessee 37232, USA; [e]Center for Mucosal Inflammation and
13 Cancer, Vanderbilt University Medical Center, Nashville, Tennessee 37232; [f]Veterans Affairs
14 Tennessee Valley Healthcare System, Nashville, Tennessee 37232; [g]Vanderbilt Institute for
15 Infection, Immunology and Inflammation, Vanderbilt University Medical Center, A5301 Medical
16 Center North, Nashville, Tennessee 37232, USA. [h]ORCID, 0000-0002-1158-8976

17

18 **Corresponding author**: Danyvid Olivares-Villagómez. Address: Vanderbilt University Medical
19 center, A5211 Medical Center North, Nashville Tennessee 37232-0001. Fax number: 615-343-
20 7392. Telephone number: 615-936-0134. email: danyvid.olivares-villagomez@vumc.org.

21

22 **Conflict of Interest**: No conflict

23

Author contributions: K.L.H., and D.O-V. designed research; K.L.H., M.J.G., K.M., A.N., and K.S. performed research; K.L.H., M.J.G., M.B.P. and D.O-V. analyzed data; K.S. and K.T.W. provided expertise with *Citrobacter rodentium* infections; K.L.H. and D.O-V. wrote the manuscript.

Acknowledgments

This work was supported by NIH grant R01DK111671 (D.O-V.); National Library of Medicine T15 LM00745 (M.J.G.); Vanderbilt Training in Cellular, Biochemical and Molecular Sciences Training Program, T32 GM008554-25 (K.G.M.); Vanderbilt Training in Gastroenterology T32 grant NIH T32 DK007673 (A.N.); and the Digestive Disease Research Center at Vanderbilt University Medical Center, NIH grant P30DK058404 (M.B.P., K.T.W., and D.O-V.). Flow cytometry experiments were performed in the VMC Flow Cytometry Shared Resource, supported by the Vanderbilt Ingram cancer Center (P30 CA068485) and the Vanderbilt Digestive Disease Research Center (DK058404). We acknowledge the Translational Pathology Shared Resource supported by NCI/NIH cancer Center Support Grant 5P30 CA68485-19 and the Mouse Metabolic Phenotyping Center Grant 2 U24 DK059637-16. We also thank the Vanderbilt Technologies for Advanced Genomics (VANTAGE) for their invaluable support.

Key words: Granzyme B; $CD4^+$ T cells; T cell differentiation; IL-17; intestinal inflammation.

Abstract: $CD4^+$ T cell activation and differentiation are important events that set the stage for proper immune responses. Many factors are involved in the activation and differentiation of T cells, and these events are tightly controlled to prevent unwanted and/or exacerbated immune responses that may harm the host. It has been well documented that granzyme B, a potent serine protease involved in cell-mediated cytotoxicity, is readily expressed by certain $CD4^+$ T cells, such as regulatory T cells and $CD4^+CD8\alpha\alpha^+$ intestinal intraepithelial lymphocytes, both of which display cytotoxicity associated with granzyme B. However, because not all $CD4^+$ T cells expressing granzyme B are cytotoxic, additional roles for this protease in $CD4^+$ T cell biology remain unknown. Here, using a combination of *in vivo* and *in vitro* approaches, we report that granzyme B-deficient $CD4^+$ T cells display increased IL-17 production. In the adoptive transfer model of intestinal inflammation, granzyme B-deficient $CD4^+$ T cells triggered a more rapid disease onset than their WT counterparts, and presented a differential transcription profile. Similar results were also observed in granzyme B-deficient mice infected with *Citrobacter rodentium*. Our results suggest that granzyme B modulates $CD4^+$ T cell differentiation, providing a new perspective into the biology of this enzyme.

66 **Introduction**

67 Granzymes are a family of serine proteases expressed by many immune cell populations.
68 There are five different granzymes in humans (A, B, H, K and M) and 11 in mice (A, B, C, D, E,
69 F, G, K, L, M and N), which differ in function and substrate specificity.[1] Most research has focused
70 on granzymes A and B due to their hallmark role in $CD8^+$ T and NK cell-mediated cytotoxicity
71 against tumor cells or virus-infected cells.[2] However, mounting evidence indicates that granzymes
72 are also involved in other processes, including inflammatory responses,[3-5] remodeling of the
73 extracellular matrix,[6] and cardiovascular disorders.[7]

74 Activated $CD4^+$ T cells express granzyme B, and some of these cells exhibit lytic activity
75 similar to $CD8^+$ T cells.[8, 9] Antigen-specific $CD4^+$ T cell lytic activity mediated by granzyme B
76 can be triggered by viral and bacterial infections.[10-12] Similarly, some tumor-infiltrating $CD4^+$ T
77 cells also present anti-tumor cytotoxicity mediated by granzyme B.[13] In addition, one of the
78 mechanisms by which regulatory $CD4^+$ T cells in humans and mice control immune responses is
79 through granzyme B-mediated cell death.[14-18]

80 After activation, $CD4^+$ T cells can differentiate into a diverse set of T helper (Th) cells
81 depending on environmental cues and transcription factors, which ultimately leads Th cells to
82 produce a specific cytokine profile.[19] In certain populations of differentiated $CD4^+$ T cells,
83 granzyme B controls $CD4^+$ T cell immune responses by initiating activation-induced cell death.[20]
84 Downregulation of granzyme B, for example when Th2 cells are cultured in the presence of
85 vasoactive intestinal peptide, reduces Th2 cell death.[20] Moreover, granzyme B expression in Th2
86 cells is enhanced by IL-10R signaling, which results in cell death.[21] These studies clearly indicate
87 that granzyme B is involved in controlling some immune $CD4^+$ T cell responses. However, it is
88 unclear whether this enzyme is actively involved during the process of Th differentiation.

89 In this report, we present data indicating that granzyme B is expressed during $CD4^+$ T cell
90 differentiation. Cells lacking granzyme B show a different cytokine profile than granzyme B-
91 competent cells, primarily presenting increased IL-17 production. Moreover, using the adoptive
92 transfer model of intestinal inflammation, we show that granzyme B-deficient $CD4^+$ T cells
93 activated *in vivo* have a different gene expression profile and display increased pathogenicity
94 relative to WT cells. Similarly, we present evidence indicating that granzyme B deficiency
95 predisposes mice to higher susceptibility to *Citrobacter rodentium* infection. These results indicate
96 that granzyme B is required for proper $CD4^+$ T cell differentiation, and in its absence, $CD4^+$ T cells
97 may acquire an aberrant phenotype characterized by increased IL-17 production and pathogenicity.
98

99 **Results**

100 **Th0 and Th1, but not Th17 $CD4^+$ T cells express granzyme B during differentiation**

101 To determine the role of granzyme B in T cell activation and differentiation, we cultured
102 naïve $CD4^+$ T cells in Th0, Th1 and Th17 differentiation conditions. One and three days after
103 culture, RNA was extracted to determine granzyme B expression relative to naïve $CD4^+$ T cells.
104 Under Th0 conditions, expression of granzyme B at day 1 displayed a slight increase above the
105 levels observed for naïve $CD4^+$ T cells (Figure 1a, top), but presented an almost three-fold increase
106 at day 3 (Figure 1a, bottom). Th1 cells expressed a 3-fold increase in granzyme B mRNA over
107 naïve T cells at day 1, which was maintained until day 3. On the other hand, $CD4^+$ T cells under
108 Th17 differentiation conditions did not induce granzyme B mRNA expression at either time point
109 (Figure 1a).

110 Around 13% of Th0 and Th1 cells expressed granzyme B intracellularly at day 5 (Figure
111 1b; see Supplemental Figure 1a for gating strategy), whereas this enzyme was not detected in Th17

112 cells, confirming the results for granzyme B mRNA expression. Although granzyme B mRNA was
113 detected at day 1 in Th1 cells, granzyme B protein was not, but the protein was conspicuously
114 expressed at day 3 and day 5 (Figure 1c). These results suggest a lag between granzyme B mRNA
115 transcription and translation. A similar granzyme B protein expression profile was detected for
116 Th0 cells (Figure 1c). On the other hand, Th17 cells did not express granzyme B at any of the time
117 points analyzed (Figure 1c). Similarly, Th2 cells did not express granzyme B (Supplemental Figure
118 2b).

119 Because Th1 and Th17 cultures contain different cytokine/antibody cocktails, and
120 granzyme B is expressed in the former, but not in the latter, we investigated what factors present
121 in these culture conditions induce or repress granzyme B expression. For this purpose, we activated
122 $CD4^+$ T cells under Th0 conditions (anti-CD3/CD28, IL-2, and irradiated spleen cells), in the
123 presence of individual factors included in Th1 and Th17 differentiation cocktails (Figure 1d). IL-
124 2 alone induced ~7.5% of $CD4^+$ T cells to express granzyme B, which was not significantly
125 different from cells activated without IL-2 (background levels), or in the presence of IL-12, IL-1β,
126 and IL-23, the last two of which are involved in Th17 differentiation. However, the Th17-inducing
127 cytokines IL-6 and TGFβ, as well as the blocking anti-IFNγ antibody, significantly ablated
128 granzyme B expression. These results indicate that $CD4^+$ T cell activation induces granzyme B
129 activation, whereas some cytokines and anti-IFNγ inhibit its expression.

130 Because most of our differentiation cultures included spleen cells as a source of APC, we
131 determined whether these cells influence granzyme B expression during $CD4^+$ T cell activation.
132 As shown in Figure 1e, $CD4^+$ T cell activation in the absence of APC (but including IL-2), resulted
133 in less than 2% of $CD4^+$ T cells expressing granzyme B, whereas irradiated spleen APC
134 significantly increased granzyme B expression.

135 Overall, these results indicate that granzyme B is expressed during Th0 and Th1
136 differentiation, with irradiated APC being an important expression-enhancing factor. On the other
137 hand, Th17 and Th2 differentiation conditions ablate granzyme B expression. This effect can be
138 attributed to IL-6, TGFβ, and anti-IFNγ.

139 As shown in Figure 1b, during Th0 and Th1 differentiation, two populations of $CD4^+$ T
140 cells can be distinguished: WT-gzmB^{pos} and WT-gzmB^{neg}. To determine whether these
141 populations present different cytokine profiles, we determined the frequencies of IFNγ- and IL-
142 17-producing cells in each of these subpopulations. Around half of Th0 WT-gzmB^{pos} expressed
143 IFNγ, whereas only around 5% of the WT-gzmB^{neg} $CD4^+$ T cells were positive for IFNγ (Figure
144 1f). Th0 cells derived from granzyme B-deficient (*Gzmb*$^{-/-}$) mice presented decreased levels of
145 IFNγ-producing cells in comparison to WT-gzmB^{pos} cells, but significantly more IFNγ$^+$ cells than
146 WT-gzmB^{neg} cells (Figure 1f). On the other hand, IL-17 production was not significantly different
147 among Th0 cells from any of the $CD4^+$ T cell populations.

148 Th1 differentiation induced high levels of IFNγ$^+$ cells in all $CD4^+$ T cell populations
149 analyzed; however, WT-gzmB^{pos} cells presented the highest levels of IFNγ$^+$ cells in comparison
150 to WT-gzmB^{neg} or cells derived from *Gzmb*$^{-/-}$ mice (Figure 1g). Interestingly, under Th1
151 conditions, cells from *Gzmb*$^{-/-}$ mice presented significantly greater levels of IL-17$^+$ cells when
152 compared to WT-gzmB^{pos} and WT-gzmB^{neg} cells (Figure 1g). These results suggest that granzyme
153 B may be involved in preventing IL-17 production when $CD4^+$ T cells are cultured under Th1
154 conditions.

155 $CD4^+$ T cells cultured in Th2 differentiation conditions, which contains anti-IFNγ, lack
156 granzyme B expression (Supplemental Figure 1b); therefore, as expected, promiscuous cytokine

157 expression in granzyme B-deficient $CD4^+$ T cells was not observed in Th2 differentiation
158 conditions (Supplemental Figure 1c).
159

160 ***In vivo* activation of granzyme B-deficient $CD4^+$ T cells results in increased pathogenicity**

161 To further understand the role of granzyme B in $CD4^+$ T cell differentiation, we adoptively
162 transferred naïve $CD4^+CD45RB^{hi}$ T cells from WT or *Gzmb*$^{-/-}$ mice into *Rag2*$^{-/-}$ recipient mice.
163 Because it is well-established that transfer of naïve $CD4^+$ T cells into immunocompromised
164 recipients results in chronic intestinal inflammation, [22, 23] this set up allows us to: 1) determine
165 whether granzyme B-deficiency alters $CD4^+$ T cell pathogenicity, and 2) whether absence of
166 granzyme B influences the cytokine profile of $CD4^+$ T cells activated *in vivo* (discussed in the next
167 section).

168 In our animal colony, transfer of naïve $CD4^+$ T cells from WT mice typically results in
169 disease symptoms by 6 weeks after transfer. However, when naïve $CD4^+$ T cells from *Gzmb*$^{-/-}$ mice
170 were transferred into *Rag2*$^{-/-}$ mice, weight loss was evident starting at 14 days after transfer, and
171 by day 21 these mice had lost around 20% of their original weight (Figure 2a). At this point, the
172 experiments were terminated to comply with our institution's animal welfare regulations. In
173 contrast, at day 21, *Rag2*$^{-/-}$ mice that received WT cells were either gaining or maintaining their
174 weight (Figure 2a). Weight loss was accompanied by increased disease severity characterized by
175 diarrhea, pilo-erection, and hunching (Figure 2b); increased intestinal pathology based on immune
176 cell infiltration, loss of goblet cells, epithelial damage and hyperplasia (Figure 2c); and donor-
177 derived $CD4^+$ T cell reconstitution (Figure 2d). To confirm that the pathogenicity observed in
178 granzyme B-deficient $CD4^+$ T cells is an intrinsic effect, we adoptively transferred naïve $CD4^+$ T
179 cells from littermate *Gzmb*$^{+/-}$ and *Gzmb*$^{-/-}$ mice into *Rag2*$^{-/-}$ recipient mice. Although disease

180 development was delayed for almost a week, *Gzmb*$^{-/-}$ mice displayed earlier disease onset and
181 increased colon pathology compared to *Gzmb*$^{+/-}$ littermate controls (Supplemental Figure 2a),
182 indicating that the pathogenicity observed is intrinsic to CD4^{+} T cells.

183 To investigate whether the recipient mice's granzyme B status is important for disease
184 development, we adoptively transferred naïve CD4^{+} T cells from WT or *Gzmb*$^{-/-}$ donor mice into
185 *Rag2*$^{-/-}$ *Gzmb*$^{-/-}$ recipient mice. Donor CD4^{+} T cells from WT mice did not cause early weight
186 loss in the double knock-out recipient mice, while CD4^{+} T cells deficient in granzyme B caused
187 similar weight loss as in *Rag2*$^{-/-}$ recipient mice (Supplemental Figure 2b and Figure 2a). Weight
188 loss in mice receiving granzyme B-deficient CD4^{+} T cells was accompanied by increased disease
189 severity (Supplemental Figure 2c), colon pathology (Supplemental Figure 3d), and donor-derived
190 CD4^{+} T cell reconstitution (Supplemental Figure 3e). Therefore, the granzyme B status in the
191 recipient mice is irrelevant for the intrinsic pathogenicity of granzyme B-deficient CD4^{+} T cells.

192 In summary, our data indicate that absence of granzyme B in CD4^{+} T cells activated *in vivo*
193 results in accelerated pathogenicity and increased cell reconstitution.

194

195 **Granzyme B-deficient CD4^{+} T cells present increased IL-17 production *in vivo*.**

196 To determine whether granzyme B deficiency results in differential CD4^{+} T cell cytokine
197 profiles *in vivo*, we adoptively transferred naïve CD4^{+}CD45RB^{hi} T cells from WT or *Gzmb*$^{-/-}$ mice
198 into *Rag2*$^{-/-}$ recipient mice. Three weeks after transfer, donor-derived cells were recovered from
199 the MLN and lamina propria and analyzed for IFNγ and IL-17 expression. As shown in Figure 3,
200 IFNγ was the predominant cytokine produced by donor CD4^{+} T cells derived from WT and *Gzmb*$^{-/-}$
201 mice, with similar levels between WT and *Gzmb*$^{-/-}$ CD4^{+} T cells (Figure 3a and 3b). However,
202 CD4^{+} T cells from *Gzmb*$^{-/-}$ donor mice presented significantly increased IL-17 production in

203 comparison to WT CD4$^+$ T cells (Figure 3a and 3b). It has been reported that pathogenesis in colitis
204 requires the development of Th17 cells expressing IFNγ.[24] As shown in Figure 3a and 3b, the
205 frequency of IL-17$^+$IFNγ$^+$ donor-derived CD4$^+$ T cells was similar among both groups in the MLN
206 and lamina propria, suggesting that these cells may not be responsible for the accelerated colitis
207 development observed. Albeit less pronounced, cytokine profiles were also similar when littermate
208 *Gzmb*$^{+/-}$ and *Gzmb*$^{-/-}$ donor mice were used (Supplemental Figure 3).
209 In summary, *in vivo* activated CD4$^+$ T cells deficient in granzyme B presented increased
210 IL-17 production. These results suggest that absence of granzyme B results in skewed *in vivo*
211 differentiation.
212
213 **Granzyme B deficient CD4$^+$ T cells present a distinct gene expression profile**
214 Because granzyme B-deficient CD4$^+$ T cells had increased IL-17 production when
215 activated *in vivo*, we investigated whether these cells presented a distinct gene expression profile
216 in comparison to *in vivo* activated CD4$^+$ T cells from WT mice. For this purpose, CD4$^+$CD45RB^{hi}
217 T cells from WT and *Gzmb*$^{-/-}$ donor mice were adoptively transferred into *Rag2*$^{-/-}$ mice. Three
218 weeks after transfer, CD4$^+$ T cells were recovered from the MLN, their RNA extracted and gene
219 expression profile determined by RNAseq. As shown in Figure 4a, WT and granzyme B-deficient
220 CD4$^+$ T cells presented significantly different gene expression profiles. Examples of genes
221 encoding transcription factors or molecules associated with gene expression upregulated in CD4$^+$
222 T cells derived from *Gzmb*$^{-/-}$ mice include Special AT-rich Binding protein (*Satb1*), a chromatin
223 remodeling protein involved in T cell development and implicated in Th2 and regulatory T cell
224 responses;[25] Krüppel-like transcription factor 13 (*Klf13*), which has been implicated in T cell
225 survival; [26] nuclear receptor subfamily 1, group D, member 1 (*Nr1d1*), which in human T cells is

226 important for circadian cycles;[27] and the Th17 master transcription factor *Rorc*. We also performed
227 gene set enrichment analysis to determine whether WT and granzyme B-deficient $CD4^+$ T cells
228 recovered from recipient mice segregated in specific groups. As indicated in Figure 4b, GSEA
229 indicated that these two $CD4^+$ T cell populations presented distinct differential gene expression
230 within several GSEA groups (Figure 4b). These results indicate that granzyme B-deficient $CD4^+$
231 T cells, in the adoptive transfer system, follow a distinct differentiation pathway compared to WT
232 $CD4^+$ T cells.

233 We validated the results generated from the RNAseq analysis by comparing the expression
234 of selected genes in naïve $CD4^+$ T cells (Figure 4c, top), and donor-derived cells recovered 21d
235 post-adoptive transfer (Figure 4c, bottom). Hallmark genes involved in Th17 responses, such as
236 *Rorc* and *Il17a*, were similarly expressed in naïve $CD4^+$ T cells, regardless of the granzyme B
237 status, but their expression was significantly increased in recovered granzyme B-deficient $CD4^+$ T
238 cells. *Ddit4*, a gene important for optimal T cell proliferation,[28] is highly expressed in T cells from
239 multiple sclerosis patients, and is important in Th17 differentiation.[29] *Ddit4* expression was 3-fold
240 higher in activated $CD4^+$ T cells derived from *Gzmb*$^{-/-}$ mice in comparison to WT $CD4^+$ T cells
241 (Figure 4c). Granzyme B-deficient $CD4^+$ T cells presented a 2-fold increase in *Il7r* expression
242 (Figure 4c), which mediates IL-7 signaling, a well-known lymphopoietic cytokine also expressed
243 in T cells undergoing homeostatic expansion.[30] Plexin D1, encoded by the *Plxnd1* gene, binds
244 semaphorins[31] and is critical for directing thymocyte migration.[32] Although the role of *Plxnd1* is
245 not well known in mature T cell biology, granzyme B-deficient $CD4^+$ T cells presented
246 approximately a 4-fold increase in expression. Interestingly, donor $CD4^+$ T cells derived from
247 *Gzmb*$^{-/-}$ mice presented decreased *Il10ra* expression in comparison to WT counterparts (Figure
248 4c).

249 In terms of IFNγ expression, the total count read average from the RNAseq analysis for
250 this gene were 2940.7±1332 and 2609.3±1348.9 (P=0.66) for cells derived from WT and *Gzmb*$^{-/-}$
251 CD4^{+} T cells, respectively, indicating that IFNγ expression is similar among the two groups. These
252 results confirm what we observed with intracellular staining for this cytokine (Figure 3).
253 Overall, these results show that in the adoptive transfer model of CD4^{+} T cell activation,
254 granzyme B deficiency results in a distinct gene expression profile, which is characterized by genes
255 relevant to Th17 differentiation and T cell proliferation.
256

257 **Granzyme B-deficient CD4^{+} T cells possess better reconstitution capability**

258 As indicated in Figure 2d, granzyme B-deficient CD4^{+} T cells showed greater
259 reconstitution in the colon than WT CD4^{+} T cells when transferred into Rag-2$^{-/-}$ recipient mice.
260 However, this observation could be due to inflammation-driven proliferation, which was more
261 prevalent in *Rag2*$^{-/-}$ mice receiving CD4^{+} T cells from *Gzmb*$^{-/-}$ mice. To further determine the
262 reconstitution potential of CD4^{+} T cells derived from WT and *Gzmb*$^{-/-}$ mice, we performed
263 competitive adoptive T cell transfer experiments. For this purpose, naïve CD4^{+} T cells from WT
264 CD45.1 and *Gzmb*$^{-/-}$ CD45.2 mice (1x10^{5} each) were adoptively co-transferred into the same *Rag2*$^{-}$
265 $^{/-}$ recipient mice. Of the total donor-derived cells obtained from the MLN, granzyme B-deficient
266 CD4^{+} T cells presented ~60% reconstitution, whereas WT-derived cells showed ~40%
267 reconstitution (Figure 5a). To determine whether increased cell reconstitution by granzyme B-
268 deficient CD4^{+} T cells correlated with increased cell division, we stained the cells for Ki67 as a
269 surrogate marker for cell division. As shown in Figure 5b, there was higher percentage of Ki67^{+}
270 cells in granzyme-B deficient donor-derived cells. To further confirm these results, we cultured
271 donor-derived cells without any stimulation, and measured their division potential by CFSE

272 dilution after 3 days. $CD4^+$ T cells from *Gzmb*$^{-/-}$ mice showed a slight increase in cell division
273 compared to cells derived from WT mice (Figure 5c).
274 We also analyzed the cytokine profile of the cells derived from the competitive adoptive
275 $CD4^+$ T cell approach. Although the IFNγ profile of co-transferred cells was similar to cells
276 transferred alone, co-transferred WT cells presented increased IL-17 production in comparison to
277 WT $CD4^+$ T cells transferred alone (Figure 5d, left and middle graphs). These results raise the
278 possibility that granzyme B-deficient $CD4^+$ T cells influenced the behavior of granzyme B-
279 competent $CD4^+$ T cells. Interestingly, co-transferred granzyme B-deficient $CD4^+$ T cells
280 displayed a higher percentage of $IFN\gamma^+IL\text{-}17^+$ cells in comparison to WT cells (Figure 5d, right
281 graph). *Rag2*$^{-/-}$ mice co-transferred with WT and $GzB^{-/-}$ $CD4^+$ T cells displayed similar weight
282 loss (Figure 5e) and colon pathology (Figure 5f) to mice transferred only with $CD4^+$ T cells from
283 *Gzmb* $^{-/-}$ mice, suggesting that the increased pathogenicity of the latter cells was maintained even
284 in the presence of granzyme-competent $CD4^+$ T cells.
285

286 **Granzyme B-deficient mice present normal cellularity and IFNγ /IL-17 production**

287 Since *in vivo* activated granzyme B-deficient $CD4^+$ T cells possess differential gene
288 expression and cytokine profiles, it is possible that these differences are also observed in naïve
289 cells. To investigate this possibility, we enumerated the $CD4^+$ T cell cellularity of spleen, MLN,
290 and IEL compartments from WT and *Gzmb*$^{-/-}$ mice. As indicated in Supplemental Figure 4a,
291 frequencies and numbers of $TCR\beta^+CD4^+$ T cells were similar among the two groups of mice. *Ex*
292 *vivo* IFNγ and IL-17 production by non-stimulated (ns) or stimulated (s) naïve $CD4^+$ T cells derived
293 from the MLN and IEL showed no distinguishable difference between cells from WT and *Gzmb*$^{-/-}$
294 mice (Supplemental Figure 4b).

295 In summary, naïve WT and *Gzmb*$^{-/-}$ animals appear to have similar CD4^{+} T cell cellularity
296 and basal IFNγ and IL-17 production in peripheral lymphoid organs and the intestines.
297
298 **Granzyme B deficiency results in increased disease severity during *Citrobacter rodentium***
299 **infection**
300 As demonstrated in the previous section, naïve *Gzmb*$^{-/-}$ mice have a normal CD4^{+} T cell
301 compartment compared to WT mice. However, because we observed that activated T cells from
302 *Gzmb*$^{-/-}$ mice became more pathogenic and had a distinct gene expression profile in the adoptive
303 transfer model of colitis, we investigated whether *Gzmb*$^{-/-}$ mice respond properly to antigenic
304 stimulus. For this purpose, we infected WT and *Gzmb* $^{-/-}$ mice with the extracellular bacterium
305 *Citrobacter rodentium*, which preferentially colonizes the colon of mice and induces an IL-17/IL-
306 22-based immune response. After infection, WT mice maintained similar weight throughout the
307 course of the experiment; however, starting at 9 days post-infection, *Gzmb*$^{-/-}$ mice lost weight,
308 reaching approximately ~20% loss of the starting weight by day 12 (Figure 6a). *Gzmb*$^{-/-}$ mice also
309 presented other signs of disease, such as diarrhea, hunched posture, and pilo-erection, which were
310 mostly absent in WT mice (Figure 6b). Despite similar colonic bacterial burden (Figure 6c), *Gzmb*$^{-}$
311 $^{/-}$ mice developed greater pathology characterized by increased infiltration and epithelial injury
312 than WT mice (Figure 6d). Analysis of cytokine production showed that in the spleen and LP of
313 infected *Gzmb*$^{-/-}$ mice, there was a significant increase in CD4^{+} T cells expressing IL-17, while
314 IFNγ production was only increased in the MLN (Figure 6e).
315 Because innate immune cells are important for the response against *C. rodentium*, we
316 investigated whether the absence of granzyme B in innate immune cells was responsible for the
317 observed increased pathology in infected *Gzmb*$^{-/-}$ mice. For this purpose, *Rag-2*$^{-/-}$ and *Rag-2*$^{-/-}$

318 *Gzmb*$^{-/-}$ mice were infected with *C. rodentium* and monitored for 14 days. Both groups of mice
319 maintained similar weights throughout the course of the experiment (Supplemental Figure 5a),
320 indicating that the effect caused by granzyme B-deficiency is most likely associated with adaptive
321 immune cells. To further confirm these results, we treated *Rag-2*$^{-/-}$ and *Rag-2*$^{-/-}$*Gzmb*$^{-/-}$ mice with
322 anti-CD40 antibodies, which induce acute intestinal inflammation in the absence of T or B cells.[33]
323 As shown in Supplemental Figure 5b, *Rag-2*$^{-/-}$ and *Rag-2*$^{-/-}$*Gzmb*$^{-/-}$ mice presented similar weight
324 loss throughout the course of the experiment.

325 Interestingly, when *Gzmb*$^{+/-}$ and *Gzmb*$^{-/-}$ littermate mice were infected with *C. rodentium*,
326 both groups displayed similar weight curves and colon colonization (Supplemental Figure 5c and
327 5d). However, there was a slight trend for increased IFNγ^{+}IL-17^{+} CD4^{+} T cells in the spleen of
328 *Gzmb*$^{-/-}$ mice (Supplemental Figure 5e).

329

330 **Discussion**

331 Granzyme B expression in CD4^{+} T cells is well-documented, and has been primarily
332 studied in the context of granzyme B/perforin-dependent regulatory T cell suppressor activity.[34]
333 However, as our data indicate, granzyme B expression appears to be a common feature among a
334 significant fraction of activated CD4^{+} T cells. Interestingly, not all differentiation conditions
335 induced granzyme B expression. For example, Th0 and Th1 cells rapidly express granzyme B
336 starting at 1-day post activation, whereas Th17 cells do not express this enzyme at any time after
337 activation. In the former conditions, expression of granzyme B is primarily driven by the presence
338 of irradiated splenocytes, indicating the possibility that cell-to-cell contact is important for
339 granzyme B expression.

340 Although none of the cytokines involved in Th1 differentiation induced granzyme B
341 expression above the levels observed with the addition of irradiated splenocytes, anti-IFNγ and
342 some cytokines present in the Th17 cocktail, such as IL-6 and TGFβ prevented the expression of
343 this enzyme, which suggests that restriction of granzyme B expression is necessary for Th17
344 polarization. Studies in cytotoxic $CD8^+$ T cells have shown that activation of these cells with anti-
345 CD3 in the presence of IL-6, but not in the presence of TGFβ, induces granzyme B expression.[35]
346 Here we show that in $CD4^+$ T cell differentiation, IL-6 does not enhance the expression of
347 granzyme B, indicating that $CD8^+$ and $CD4^+$ T cells possess different mechanisms for modulating
348 granzyme B production.

349 Granzyme B expression may not only be limited during the initial $CD4^+$ T cell priming and
350 differentiation. For example, TGFβ is known for its role in regulatory T cell differentiation, and
351 some of these cells require granzyme B for their suppressor functions. However, as our results
352 indicate, TGFβ ablates expression of this enzyme, suggesting that regulatory T cells must acquire
353 granzyme B expression during post-priming events. Similarly, a fraction of effector $CD4^+$ T cells
354 that migrate into the intestinal intraepithelial lymphocyte compartment acquire granzyme B
355 expression after transcriptional reprogramming.[36]

356 One of the most intriguing questions is: Why do $CD4^+$ T cells express granzyme B during
357 Th0/Th1 activation and differentiation? During *in vitro* Th0/Th1 differentiation, WT-gzmB^{pos} and
358 WT-gzmB^{neg} cells have distinct IFNγ profiles, suggesting that these cells may represent different
359 lineages and that the activity of granzyme B influences their outcome. This is better exemplified
360 when analyzing granzyme B-deficient $CD4^+$ T cells, where *in vivo* and *in vitro* activation skew the
361 cells towards an IL-17-producing phenotype, with a distinct gene expression signature. We
362 postulate that granzyme B-deficient IL-17^+ cells represent a lineage of cells that underwent

363 aberrant differentiation. Therefore, expression of granzyme B during Th0/Th1 activation serves as
364 a checkpoint for proper $CD4^+$ T cell differentiation, preventing IL-17 production and increased
365 pathology. These observations have important significance because it has been reported that allelic
366 variants of granzyme B correlate with autoimmune disorders,[37-39] raising the possibility that in
367 certain $CD4^+$ T cell-mediated disorders, lack of proper granzyme B function increases the
368 probability of improper differentiation and increased pathogenesis potential. If this idea is correct,
369 then WT-gzmB^{pos} $CD4^+$ T cells may represent cells in which the differentiation signals have the
370 potential to skew cells into an unwanted phenotype, and granzyme B expression in these cells
371 ensures the correct differentiation process.

372 We have shown that adoptive transfer of $CD4^+$ T cells derived from non-littermate (Figure
373 2) and littermate (Supplemental Figure 2a) mice resulted in increased pathogenicity and IL-17
374 production, which argues that granzyme B deficiency has an intrinsic effect in $CD4^+$ T cells.
375 However, the host's environment also influences the pathogenicity and IL-17 production of
376 granzyme B-deficient $CD4^+$ T cells. For example, infection of *Gzmb*$^{-/-}$ mice with *C. rodentium*
377 resulted in more severe disease with increased IL-17 production relative to WT mice (Figure 6);
378 however, this effect was not observed in infected *Gzmb*$^{+/-}$ and *Gzmb*$^{-/-}$ littermate mice
379 (Supplemental Figure 5c-5e). This observation suggests that granzyme B deficiency in $CD4^+$ T
380 cells is necessary but not sufficient for their associated increased IL-17 production and
381 pathogenicity. One potential factor that may be responsible for controlling the pathogenicity of
382 granzyme B-deficient $CD4^+$ T cells may be the microbiota present in granzyme B-competent mice.
383 We are currently investigating this interesting hypothesis.

384 Granzyme B activity in lymphocyte development and/or differentiation has been
385 previously reported.[40] These authors showed that granzyme A and B are important for the

386 development of a subset of TCR^{neg} intestinal intraepithelial lymphocytes known for the expression
387 of intracellular CD3γ. Development of these cells requires granzyme B to cleave and inactivate
388 the intracellular domain of Notch1. This raises the interesting possibility that during CD4$^+$ T cell
389 differentiation, granzyme B prevents unwanted phenotypes by disrupting signals coming from the
390 environment, such those provided by Notch and its ligands, which are known to influence CD4$^+$ T
391 cell differentiation.[41] Our observation that granzyme B expression was increased in the presence
392 of irradiated splenocytes supports this hypothesis. We are currently investigating what signals
393 derived from APC enhance granzyme B expression.

394 It has been reported that granzyme B-deficient CD4$^+$CD25$^-$ T cells used in murine models
395 of graft versus host disease (GVHD) induced faster disease onset with increased lethality in
396 comparison to their WT counterparts.[42] Although this group did not provide a mechanistic
397 explanation for the increased pathogenicity observed, they suggested that increased proliferation
398 and decreased cell death may be involved. According to our data, we believe that in the GVHD
399 model, differential proliferation and survival of granzyme B-deficient CD4$^+$ T cells are the result
400 of aberrant CD4$^+$ T cell differentiation, which allows escape of highly pathogenic clones. Further
401 investigations in the GVHD model are needed to test this hypothesis.

402 In summary, granzyme B has been known for its role in cell mediated-cytotoxicity, and
403 while many groups have reported potential extracellular roles for this enzyme,[43] here we present
404 *in vitro* and *in vivo* evidence supporting a novel intrinsic function for granzyme B during CD4$^+$ T
405 cell differentiation. Although many questions remain to be answered regarding how granzyme B
406 is involved in this process, our results provide a strong foundation for a better understanding of
407 the function of this enzyme in CD4$^+$ T cell biology.
408

409 **Methods**

410 *Mice*. C57BL/6J and C57BL/6J.CD45.1 mice were originally purchased from The Jackson
411 Laboratory (000664, and 002014 respectively) and have been maintained and acclimated in our
412 colony for several years. Granzyme B (*Gzmb*)$^{-/-}$ mice were kindly provided by Dr. Xuefang Cao.
413 Littermate mice were generated by crossing *Gzmb*$^{-/-}$ with WT mice; F1 males (*Gzmb*$^{+/-}$) were
414 subsequently crossed to *Gzmb*$^{-/-}$ female mice to obtain *Gzmb*$^{+/-}$ and *Gzmb*$^{-/-}$ mice. CD57BL/6J
415 *Rag2*$^{-/-}$ mice were kindly provided by Dr. Luc Van Kaer. *Rag2*$^{-/-}$*Gzmb*$^{-/-}$ were generated in our
416 colony. All mice were between 6 to 10 weeks of age at the time of experimentation. Male and
417 female mice were used for all experiments. Mice were maintained in accordance with the
418 Institutional Animal Care and Use Committee at Vanderbilt University.

419

420 *Reagents and flow cytometry.* Fluorochrome-coupled anti-mouse CD4 (GK1.5), CD8α (53-6.7),
421 CD45RB (C363.16A), granzyme B (NGZB), IFNγ (XMG1.2), IL-17a (TC11-18H10), Ki67
422 (solA15), TCRβ (H57-597) and ghost viability dyes were purchased from ThermoFisher, BD
423 Bioscences or Tonbo. Biotinylated anti-CD8α (53-1.7) and CD19 (1D3) antibodies were
424 purchased from Tonbo. The Invitrogen Vybrant CFDA SE cell tracer kit was purchased from
425 ThermoFisher Scientific. Anti-CD40 antibody was purchased from BioXcell. Surface cell staining
426 was performed following conventional techniques. For intracellular cytokine staining, cells were
427 stimulated with PMA and ionomycin in the presence of Golgi Stop (BD Biosciences) for 4hr prior
428 to staining. Extracellular markers were stained, cells were fixed briefly with 2% paraformaldehyde,
429 followed by permeabilization and intracellular staining. For intracellular cytokine and granzyme
430 B staining, the BD Cytofix/Cytoperm kit was used according to the manufacturer's instructions.
431 For intracellular Ki67 staining, the eBioscience transcription factor staining buffer set was used

432 according to the manufacturer's instructions. All stained samples were acquired using BD FACS
433 Canto II, 3- or 4-Laser Fortessa, or 5-Laser LSR II flow cytometers (BD Bioscences). Data were
434 analyzed using FlowJo software (Tree Star).
435
436 *Lymphocyte isolation*. Spleen and MLN lymphocytes were isolated by conventional means. IEL
437 and LP cells were isolated by mechanical disruption as previously reported.[44] Briefly, after
438 flushing the intestinal contents with cold HBSS and removing excess mucus, the intestines were
439 cut into small pieces (~1 cm long) and shaken for 45 minutes at 37°C in HBSS supplemented with
440 5% fetal bovine serum and 2 mM EDTA. Supernatants were recovered and cells isolated using a
441 discontinuous 40/70% Percoll (General Electric) gradient. To obtain lamina propria lymphocytes,
442 intestinal tissue was recovered and digested with collagenase (187.5 U/ml, Sigma) and DNase I
443 (0.6 U /ml, Sigma). Cells were isolated using a discontinuous 40/70% Percoll gradient.
444
445 In vitro *CD4 T cell activation/differentiation.* Naïve CD4 T cells were isolated from the spleens of
446 the indicated mice by magnetic sorting using the Miltenyi or StemCell Technologies naïve $CD4^+$
447 T cell isolation kits according to the manufacturer's instructions. Splenocytes or MLN cells used
448 as APC were incubated for 1hr at 37°C, non-adherent cells were removed, adherent cells were
449 washed and resuspended in complete RPMI, and irradiated with 7 Gy (700 rads). $5x10^5$ $CD4^+$ T
450 cells with or without $5x10^5$ irradiated APC were incubated in the presence of plate bound anti-
451 CD3 (5μg/ml) and soluble anti-CD28 (2.5μg/ml), for the indicated times, under the following
452 conditions: Th0 (10ng/mL IL-2), Th1 (10ng/mL IL-2, 20ng/mL IL-12, and 10μg/mL anti-IL-4) ,
453 Th17 (5ng/mL TGFβ, 20ng/mL IL-6, 10ng/mL IL-1β, 10ng/mL IL-23, 10μg/mL anti-IL-4, and
454 10μg/mL anti-IFNγ), and Th2 (10ng/mL IL-4, 2μg/mL anti-IFNγ, and 2μg/mL anti IL-12).

455

456 *Adoptive transfer of naïve CD4 T cells*. Splenocytes from WT or *Gzmb*$^{-/-}$ mice were depleted of
457 CD19^{+} and CD8α^{+} cells using magnetic bead sorting (Miltenyi). Enriched cells were stained with
458 antibodies directed against TCRβ, CD4 and CD45RB, and naïve CD4^{+} T cells were sorted as
459 CD4^{+}CD45RB^{hi} using a FACSAria III at the Flow Cytometry Shared Resource at VUMC. 1x10^{5}
460 cells were adoptively transferred into the indicated recipient mice. Starting weight was determined
461 prior to injection. Mice were monitored and weighed weekly. At the end time point, mice were
462 sacrificed and donor-derived cells were isolated from the indicated organs or tissues. Colon
463 histopathology was performed in a blind fashion by a GI pathologist (MBP), following established
464 parameters.[45] For competitive transfer experiments, 1x10^{5} CD4^{+}CD45RB^{hi} cells from both WT-
465 CD45.1 and *Gzmb*$^{-/-}$ CD45.2 mice were adoptively co-transferred into *Rag2*$^{-/-}$ mice and analyzed
466 as indicated above.

467

468 *Transcription profile analysis.* For gene expression analysis, TCRβ^{+}CD4^{+} T cells were purified by
469 flow cytometry from a pool of MLN cells comprised of 1 male and 1 female animal with similar
470 disease progression 21 days after adoptive transfer. RNA was isolated using the RNeasy micro kit
471 (Qiagen). cDNA library preparation and RNAseq was performed by the VANTAGE Core at
472 VUMC on an Illumina NovaSeq 6000 (2 x 150 base pair, paired-end reads). The tool Salmon[46]
473 was used for quantifying the expression of RNA transcripts. The R project software along with the
474 edgeR method[47] was used for differential expression analysis. For gene set enrichment analysis
475 (GSEA), RNAseq data was ranked according to the t-test statistic. The gene sets curated (C2), GO
476 (C5), immunological signature collection (C7) and hallmarks of cancer (H) of the Molecular

477 Signatures Database (MSigDB) were used for enrichment analysis. GSEA enrichment plots were
478 generated using the GSEA software[48] from the Broad Institute with 1000 permutations.
479
480 *Real time PCR*. For *in vitro* analysis, RNA was extracted from MACS-enriched, differentiated
481 $CD4^+$ T cells at day 1 and 3 of culture. For *in vivo* analysis, RNA was isolated from flow cytometry
482 purified donor-derived $TCR\beta^+CD4^+$ T cells as described above. cDNA was synthesized using the
483 RT2 First Strand kit (Qiagen). Real time PCR was performed using RT2 SYBR Green Mastermix
484 (Qiagen) on an Applied BioSystems Proflex PCR cycler. All primers were purchased from Qiagen.
485
486 Citrobacter rodentium *infection*. Seven-week old female WT and *Gzmb*$^{-/-}$ or *Gzmb*$^{+/-}$ and *Gzmb*$^{-/-}$
487 littermate animals were infected with *C. rodentium* as previously described[49]. Briefly, mice were
488 infected with $5x10^8$ CFU exponentially grown bacteria by oral gavage. Starting weight was
489 determined prior to gavage. Mice were monitored and weighed daily for 14d. At the end time
490 point, cells were isolated from the indicated organs or tissues. Cellularity was determined,
491 intracellular cytokine staining was performed, and colon histopathology was performed in a blind
492 fashion by a GI pathologist (MBP) as previously described.[50]
493
494 *Anti-CD40 disease induction*. *Rag-2*$^{-/-}$ and *Rag-2*$^{-/-}$*Gzmb*$^{-/-}$ mice were injected i.p. with
495 150μg/mouse of anti-CD40 (BioXcell). Mice were monitored and weighed for daily for 7 days.
496
497 **References**

498 1. Anthony DA, Andrews DM, Watt SV, Trapani JA, Smyth MJ. Functional dissection of the
499 granzyme family: cell death and inflammation. *Immunol Rev* 2010; **235**(1)**:** 73-92.
500

501 2. Chowdhury D, Lieberman J. Death by a thousand cuts: granzyme pathways of programmed
502 cell death. *Annu Rev Immunol* 2008; **26:** 389-420.
503
504 3. Afonina IS, Cullen SP, Martin SJ. Cytotoxic and non-cytotoxic roles of the CTL/NK
505 protease granzyme B. *Immunol Rev* 2010; **235**(1)**:** 105-116.
506
507 4. Wensink AC, Hack CE, Bovenschen N. Granzymes regulate proinflammatory cytokine
508 responses. *J Immunol* 2015; **194**(2)**:** 491-497.
509
510 5. Kumar AA, Delgado AG, Piazuelo MB, Van Kaer L, Olivares-Villagomez D. Innate
511 CD8alphaalpha(+) lymphocytes enhance anti-CD40 antibody-mediated colitis in mice.
512 *Immun Inflamm Dis* 2017; **5**(2)**:** 109-123.
513
514 6. Parkinson LG, Toro A, Zhao H, Brown K, Tebbutt SJ, Granville DJ. Granzyme B mediates
515 both direct and indirect cleavage of extracellular matrix in skin after chronic low-dose
516 ultraviolet light irradiation. *Aging Cell* 2015; **14**(1)**:** 67-77.
517
518 7. Chamberlain CM, Ang LS, Boivin WA, Cooper DM, Williams SJ, Zhao H *et al.* Perforin-
519 independent extracellular granzyme B activity contributes to abdominal aortic aneurysm.
520 *Am J Pathol* 2010; **176**(2)**:** 1038-1049.
521
522 8. Lancki DW, Hsieh CS, Fitch FW. Mechanisms of lysis by cytotoxic T lymphocyte clones.
523 Lytic activity and gene expression in cloned antigen-specific CD4+ and CD8+ T
524 lymphocytes. *J Immunol* 1991; **146**(9)**:** 3242-3249.
525
526 9. Ebnet K, Chluba-de Tapia J, Hurtenbach U, Kramer MD, Simon MM. In vivo primed
527 mouse T cells selectively express T cell-specific serine proteinase-1 and the proteinase-
528 like molecules granzyme B and C. *Int Immunol* 1991; **3**(1)**:** 9-19.
529
530 10. Sun Q, Burton RL, Pollok KE, Emanuel DJ, Lucas KG. CD4(+) Epstein-Barr virus-specific
531 cytotoxic T-lymphocytes from human umbilical cord blood. *Cell Immunol* 1999; **195**(2)**:**
532 81-88.
533
534 11. Canaday DH, Wilkinson RJ, Li Q, Harding CV, Silver RF, Boom WH. CD4(+) and CD8(+)
535 T cells kill intracellular Mycobacterium tuberculosis by a perforin and Fas/Fas ligand-
536 independent mechanism. *J Immunol* 2001; **167**(5)**:** 2734-2742.
537
538 12. Yasukawa M, Ohminami H, Yakushijin Y, Arai J, Hasegawa A, Ishida Y *et al.* Fas-
539 independent cytotoxicity mediated by human CD4+ CTL directed against herpes simplex
540 virus-infected cells. *J Immunol* 1999; **162**(10)**:** 6100-6106.
541
542 13. Dorothee G, Vergnon I, Menez J, Echchakir H, Grunenwald D, Kubin M *et al.* Tumor-
543 infiltrating CD4+ T lymphocytes express APO2 ligand (APO2L)/TRAIL upon specific
544 stimulation with autologous lung carcinoma cells: role of IFN-alpha on APO2L/TRAIL
545 expression and -mediated cytotoxicity. *J Immunol* 2002; **169**(2)**:** 809-817.
546

547 14. Grossman WJ, Verbsky JW, Tollefsen BL, Kemper C, Atkinson JP, Ley TJ. Differential
548 expression of granzymes A and B in human cytotoxic lymphocyte subsets and T regulatory
549 cells. *Blood* 2004; **104**(9)**:** 2840-2848.
550
551 15. Koonpaew S, Shen S, Flowers L, Zhang W. LAT-mediated signaling in CD4+CD25+
552 regulatory T cell development. *J Exp Med* 2006; **203**(1)**:** 119-129.
553
554 16. Kawamura K, Kadowaki N, Kitawaki T, Uchiyama T. Virus-stimulated plasmacytoid
555 dendritic cells induce CD4+ cytotoxic regulatory T cells. *Blood* 2006; **107**(3)**:** 1031-1038.
556
557 17. Price JD, Schaumburg J, Sandin C, Atkinson JP, Lindahl G, Kemper C. Induction of a
558 regulatory phenotype in human CD4+ T cells by streptococcal M protein. *J Immunol* 2005;
559 **175**(2)**:** 677-684.
560
561 18. Gondek DC, Lu LF, Quezada SA, Sakaguchi S, Noelle RJ. Cutting edge: contact-mediated
562 suppression by CD4+CD25+ regulatory cells involves a granzyme B-dependent, perforin-
563 independent mechanism. *J Immunol* 2005; **174**(4)**:** 1783-1786.
564
565 19. Zhu J, Yamane H, Paul WE. Differentiation of effector CD4 T cell populations (*). *Annu*
566 *Rev Immunol* 2010; **28:** 445-489.
567
568 20. Sharma V, Delgado M, Ganea D. Granzyme B, a new player in activation-induced cell
569 death, is down-regulated by vasoactive intestinal peptide in Th2 but not Th1 effectors. *J*
570 *Immunol* 2006; **176**(1)**:** 97-110.
571
572 21. Coomes SM, Kannan Y, Pelly VS, Entwistle LJ, Guidi R, Perez-Lloret J *et al.* CD4(+) Th2
573 cells are directly regulated by IL-10 during allergic airway inflammation. *Mucosal*
574 *immunology* 2017; **10**(1)**:** 150-161.
575
576 22. Powrie F, Correa-Oliveira R, Mauze S, Coffman RL. Regulatory interactions between
577 CD45RBhigh and CD45RBlow CD4+ T cells are important for the balance between
578 protective and pathogenic cell-mediated immunity. *J Exp Med* 1994; **179**(2)**:** 589-600.
579 PMC2191378.
580
581 23. Powrie F, Leach MW, Mauze S, Menon S, Caddle LB, Coffman RL. Inhibition of Th1
582 responses prevents inflammatory bowel disease in scid mice reconstituted with CD45RBhi
583 CD4+ T cells. *Immunity* 1994; **1**(7)**:** 553-562.
584
585 24. Harbour SN, Maynard CL, Zindl CL, Schoeb TR, Weaver CT. Th17 cells give rise to Th1
586 cells that are required for the pathogenesis of colitis. *Proc Natl Acad Sci U S A* 2015;
587 **112**(22)**:** 7061-7066.
588
589 25. Zelenka T, Spilianakis C. SATB1-mediated chromatin landscape in T cells. *Nucleus* 2020;
590 **11**(1)**:** 117-131.
591

592 26. Zhou M, McPherson L, Feng D, Song A, Dong C, Lyu SC *et al.* Kruppel-like transcription
593 factor 13 regulates T lymphocyte survival in vivo. *J Immunol* 2007; **178**(9)**:** 5496-5504.
594
595 27. Bollinger T, Leutz A, Leliavski A, Skrum L, Kovac J, Bonacina L *et al.* Circadian clocks
596 in mouse and human CD4+ T cells. *PLoS One* 2011; **6**(12)**:** e29801.
597
598 28. Reuschel EL, Wang J, Shivers DK, Muthumani K, Weiner DB, Ma Z *et al.* REDD1 Is
599 Essential for Optimal T Cell Proliferation and Survival. *PLoS One* 2015; **10**(8)**:** e0136323.
600
601 29. Zhang F, Liu G, Li D, Wei C, Hao J. DDIT4 and Associated lncDDIT4 Modulate Th17
602 Differentiation through the DDIT4/TSC/mTOR Pathway. *J Immunol* 2018; **200**(5)**:** 1618-
603 1626.
604
605 30. Fry TJ, Mackall CL. The many faces of IL-7: from lymphopoiesis to peripheral T cell
606 maintenance. *J Immunol* 2005; **174**(11)**:** 6571-6576.
607
608 31. Carvalheiro T, Rafael-Vidal C, Malvar-Fernandez B, Lopes AP, Pego-Reigosa JM,
609 Radstake T *et al.* Semaphorin4A-Plexin D1 Axis Induces Th2 and Th17 While Represses
610 Th1 Skewing in an Autocrine Manner. *Int J Mol Sci* 2020; **21**(18).
611
612 32. Choi YI, Duke-Cohan JS, Ahmed WB, Handley MA, Mann F, Epstein JA *et al.* PlexinD1
613 glycoprotein controls migration of positively selected thymocytes into the medulla.
614 *Immunity* 2008; **29**(6)**:** 888-898.
615
616 33. Uhlig HH, McKenzie BS, Hue S, Thompson C, Joyce-Shaikh B, Stepankova R *et al.*
617 Differential activity of IL-12 and IL-23 in mucosal and systemic innate immune pathology.
618 *Immunity* 2006; **25**(2)**:** 309-318.
619
620 34. Cao X, Cai SF, Fehniger TA, Song J, Collins LI, Piwnica-Worms DR *et al.* Granzyme B
621 and perforin are important for regulatory T cell-mediated suppression of tumor clearance.
622 *Immunity* 2007; **27**(4)**:** 635-646.
623
624 35. Huber M, Heink S, Grothe H, Guralnik A, Reinhard K, Elflein K *et al.* A Th17-like
625 developmental process leads to CD8(+) Tc17 cells with reduced cytotoxic activity. *Eur J*
626 *Immunol* 2009; **39**(7)**:** 1716-1725.
627
628 36. Mucida D, Husain MM, Muroi S, van Wijk F, Shinnakasu R, Naoe Y *et al.* Transcriptional
629 reprogramming of mature CD4(+) helper T cells generates distinct MHC class II-restricted
630 cytotoxic T lymphocytes. *Nat Immunol* 2013; **14**(3)**:** 281-289.
631
632 37. Jin Y, Birlea SA, Fain PR, Gowan K, Riccardi SL, Holland PJ *et al.* Variant of TYR and
633 autoimmunity susceptibility loci in generalized vitiligo. *The New England journal of*
634 *medicine* 2010; **362**(18)**:** 1686-1697.
635

38. Li S, Yao W, Pan Q, Tang X, Zhao S, Wang W *et al.* Association analysis revealed one susceptibility locus for vitiligo with immune-related diseases in the Chinese Han population. *Immunogenetics* 2015; **67**(7)**:** 347-354.

39. Shen C, Gao J, Sheng Y, Dou J, Zhou F, Zheng X *et al.* Genetic Susceptibility to Vitiligo: GWAS Approaches for Identifying Vitiligo Susceptibility Genes and Loci. *Front Genet* 2016; **7:** 3.

40. Ettersperger J, Montcuquet N, Malamut G, Guegan N, Lopez-Lastra S, Gayraud S *et al.* Interleukin-15-Dependent T-Cell-like Innate Intraepithelial Lymphocytes Develop in the Intestine and Transform into Lymphomas in Celiac Disease. *Immunity* 2016; **45**(3)**:** 610-625.

41. Amsen D, Helbig C, Backer RA. Notch in T Cell Differentiation: All Things Considered. *Trends Immunol* 2015; **36**(12)**:** 802-814.

42. Du W, Leigh ND, Bian G, O'Neill RE, Mei L, Qiu J *et al.* Granzyme B-Mediated Activation-Induced Death of CD4+ T Cells Inhibits Murine Acute Graft-versus-Host Disease. *J Immunol* 2015; **195**(9)**:** 4514-4523.

43. Boivin WA, Cooper DM, Hiebert PR, Granville DJ. Intracellular versus extracellular granzyme B in immunity and disease: challenging the dogma. *Laboratory investigation; a journal of technical methods and pathology* 2009; **89**(11)**:** 1195-1220.

44. Nazmi A, Greer MJ, Hoek KL, Piazuelo MB, Weitkamp J, Olivares-Villagomez D. Osteopontin and iCD8alpha cells promote intestinal intraepithelial lymphocyte homeostasis. *J Immunol* 2020; **In press**.

45. Aranda R, Sydora BC, McAllister PL, Binder SW, Yang HY, Targan SR *et al.* Analysis of intestinal lymphocytes in mouse colitis mediated by transfer of CD4+, CD45RBhigh T cells to SCID recipients. *J Immunol* 1997; **158**(7)**:** 3464-3473.

46. Patro R, Duggal G, Love MI, Irizarry RA, Kingsford C. Salmon provides fast and bias-aware quantification of transcript expression. *Nature methods* 2017; **14**(4)**:** 417-419.

47. Robinson MD, McCarthy DJ, Smyth GK. edgeR: a Bioconductor package for differential expression analysis of digital gene expression data. *Bioinformatics* 2010; **26**(1)**:** 139-140.

48. Subramanian A, Tamayo P, Mootha VK, Mukherjee S, Ebert BL, Gillette MA *et al.* Gene set enrichment analysis: a knowledge-based approach for interpreting genome-wide expression profiles. *Proc Natl Acad Sci U S A* 2005; **102**(43)**:** 15545-15550.

49. Olivares-Villagomez D, Algood HM, Singh K, Parekh VV, Ryan KE, Piazuelo MB *et al.* Intestinal epithelial cells modulate CD4 T cell responses via the thymus leukemia antigen. *J Immunol* 2011; **187**(8)**:** 4051-4060.

682 50. Singh K, Gobert AP, Coburn LA, Barry DP, Allaman M, Asim M *et al.* Dietary Arginine
683 Regulates Severity of Experimental Colitis and Affects the Colonic Microbiome. *Front*
684 *Cell Infect Microbiol* 2019; **9:** 66.
685
686

687

688 **Figure legends**

689

690 **Figure 1**. Granzyme B expression during T cell differentiation. (a) Naïve $CD4^+$ T cells from WT
691 mice were cultured in the presence of plate-bound anti-CD3 and soluble anti-CD28 under the
692 indicated differentiation conditions, and in the absence of irradiated splenocytes. At day 1 (top)
693 and 3 (bottom), cells were recovered, RNA extracted and granzyme B mRNA expression
694 determined. Naïve $CD4^+$ T cells without stimulation were used as reference. (b) Intracellular
695 granzyme B in cells cultured as in (a), but in the presence of irradiated splenocytes. Left,
696 representative dot plot (see Supplemental Figure 1a for gating strategy). Right, data summary. (c)
697 Granzyme B expression in cells cultured in Th0, Th1 and Th17 conditions in the presence of
698 irradiated splenocytes at different time points. (d) Cells cultured in Th0 conditions in the
699 presence of irradiated splenocytes and the indicated individual cytokines, harvested 5 days after
700 culture. (e) Cells cultured with IL-2, with or without irradiated splenocytes (APC). (f) and (g),
701 intracellular IFNγ and IL-17 staining of WT and *Gzmb*$^{-/-}$ $CD4^+$ T cells cultured in Th0 or Th1
702 conditions, respectively, in the presence of irradiated splenocytes. Top, intracellular IFNγ and
703 IL-17 staining of representative concatenated plots; bottom, data summary. Each dot represents
704 an individual sample. Data are representative of at least 3 independent experiments, performed in
705 triplicate. n=6. For (d), (f) and (g), *P<0.05; **P<0.01; ***P<0.001; ****P<0.001, One-way
706 ANOVA; For (e), ***P<0.001, Student's t test.

707

708 **Figure 2**. *In vivo* activated granzyme B-deficient $CD4^+$ T cells display increased pathogenicity.
709 $1x10^5$ $CD4^+CD45RB^{hi}$ T cells from WT or *Gzmb*$^{-/-}$ donor mice were adoptively transferred into
710 *Rag2*$^{-/-}$ recipient mice. (a) Mice were weighed weekly, and (b) monitored for signs of disease.
711 Twenty-one days after transfer, (c) colon pathology was scored (left, representative micrographs;
712 right, data summary), and (d) donor-cell reconstitution of the IEL compartment in the colon was
713 determined. For (a), dotted lines represent untreated *Rag2*$^{-/-}$ mice. Each dot represents an
714 individual mouse. Data are representative of at least 3 independent experiments. n=8-10.
715 **P<0.01; ***P<0.001; ****P<0.0001; Student's t-test.

716

717 **Figure 3**. Granzyme B-deficient $CD4^+$ T cells display skewed IL-17 differentiation *in vivo.*
718 $1x10^5$ $CD4^+CD45RB^{hi}$ T cells from WT or *Gzmb*$^{-/-}$ donor mice were adoptively transferred into

719 *Rag2*$^{-/-}$ recipient mice. Three weeks after transfer, donor-derived cells were recovered from (a)
720 MLN, and (b) lamina propria, and their IFNγ/IL-17 profile was determined by intracellular
721 staining. Dot plots indicate a representative sample. Live, TCRβ^{+}CD4^{+} cells are displayed.
722 Graphs represent the summary. Each dot indicates an individual mouse. For MLN, n=11-13; for
723 lamina propria, n=7-11. Data are representative of at least 3 independent experiments. **P<0.01;
724 ****P<0.001. Student's t-Test.
725
726 **Figure 4**. Granzyme B-deficient CD4^{+} T cells activated *in vivo* display a distinct gene expression
727 profile. 1x10^{5} CD4^{+}CD45RB^{hi} T cells from WT or *Gzmb*$^{-/-}$ donor mice were adoptively
728 transferred into *Rag2*$^{-/-}$ recipient mice. Three weeks after transfer, donor-derived cells were
729 recovered from the MLN, sorted for live TCRβ^{+}CD4^{+}, their RNA isolated and sequenced. (a)
730 Representative heat map. (b) Representative gene set enrichment analysis. The green line on the
731 plots indicate the enrichment score; the black lines show where the genes related to the pathway
732 are located in the ranking; the legend at the bottom indicates whether the expression of the genes
733 correlate more with CD4^{+} T cells derived from WT or *Gzmb*$^{-/-}$ mice. (c) Real-time PCR
734 validation of selected genes. For day 0, n=2; for day 21, n=3-6. *P<0.05; **P<0.01. Student's t-
735 Test.
736
737 **Figure 5**. Granzyme B-deficient CD4^{+} T cells present greater *in vivo* reconstitution.
738 1x10^{5} CD4^{+}CD45RB^{hi} T cells from WT (CD45.1) and *Gzmb*$^{-/-}$ (CD45.2) donor mice were co-
739 transferred into the same *Rag2*$^{-/-}$ recipient mice. As controls, cells from the same donors were
740 independently transferred into *Rag2*$^{-/-}$ recipient mice. Three weeks after transfer, (a) MLN
741 reconstitution (right, representative dot plot displaying live, TCRβ^{+}CD4^{+} cells; left, summary),
742 and (b) Ki67 staining were determined. (c) *In vitro* proliferation potential measured by CFSE
743 dilution. Histograms indicate representative samples. Gray, WT; Red, *Gzmb*$^{-/-}$. The gates indicate
744 CFSE-negative cells; graph represents summary. (d) IFNγ/IL-17 production was determined
745 from cells as in (a); graphs represent single IFNγ^{+} or IL-17^{+} (left and middle, respectively), and
746 IFNγ^{+}IL-17^{+} cells (right). (e) *Rag2*$^{-/-}$ mice that received CD4^{+} T cells from both WT/*Gzmb*$^{-/-}$ or
747 only *Gzmb*$^{-/-}$ mice were weighed weekly. (f) Colon pathology was determined 3 weeks post
748 transfer. For (a) n=11; (b) n=9; (c) n=5; (d) n=4-9; (e), n=5-9. Each dot represents an individual

749 mouse. Data are representative of at least 2 independent experiments. *P<0.05; **P<0.01;
750 ***P<0.001; ****P<0.0001. For (a) and (b) Student's t-Test; for (d) One-Way ANOVA.
751
752 **Figure 6.** Granzyme B-deficient mice present severe disease after *C. rodentium* infection.
753 Indicated mice were orogastrically infected with *C. rodentium* ($5x10^8$ CFU/mouse) and
754 monitored for (a) weight change, and (b) signs of disease. At 14 days post infection, colons were
755 dissected, (c) colonization/g of colon was determined, and (d) pathology scored as indicated in
756 the Methods section; left, representative micrographs (200X magnification); right, data
757 summary. (e) $CD4^+$ T cell IFNγ and IL-17 expression in the indicated organs was determined.
758 Cells were non-stimulated (ns) or stimulated (s) for 4 h with PMA/ionomycin. Each dot
759 represents an individual mouse. For (a-d), n=7-9; for (e), 3-5. Data are representative of at least 3
760 independent experiments. For (a): **P<0.01; ***P<0.01; ****P<0.001; Student's t-Test. For (b):
761 ****P<0.001; Student's t-Test. For (d) and (e): *P<0.05; **P<0.01; One-way ANOVA.

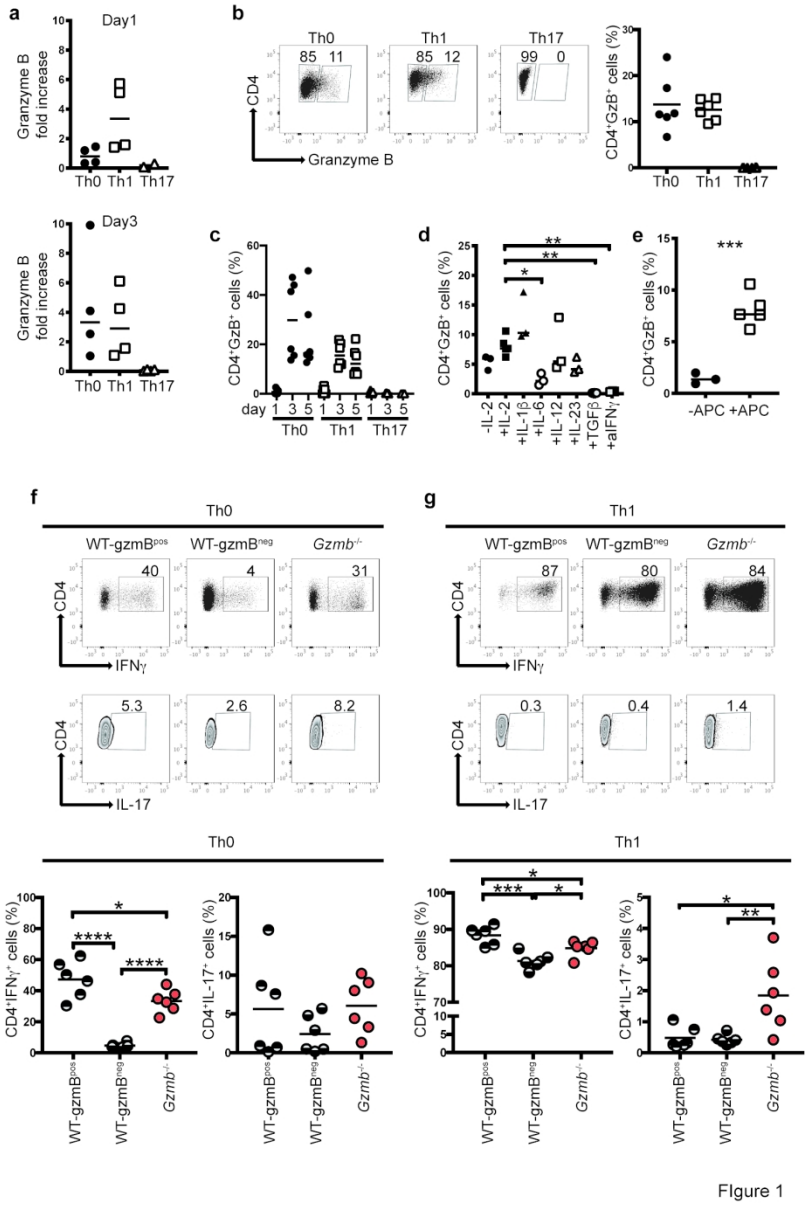

FIgure 1

Figure 1

167x246mm (240 x 240 DPI)

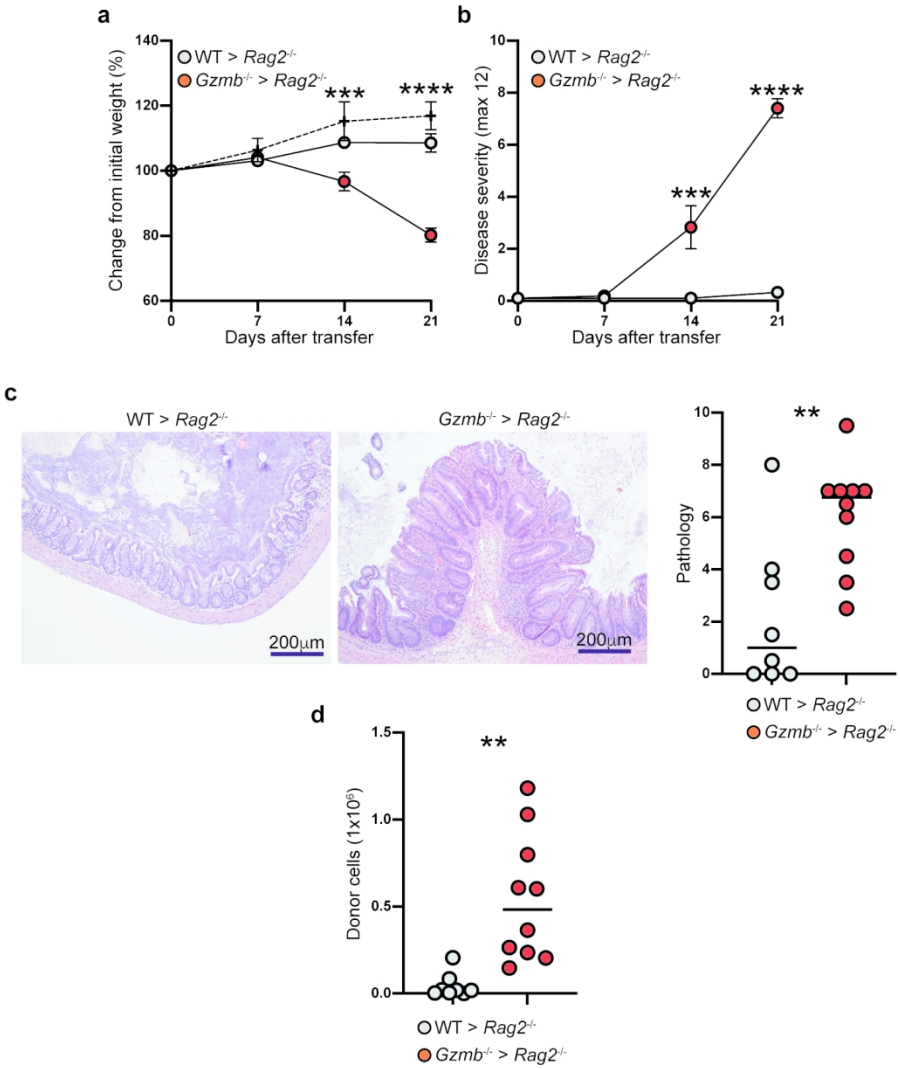

Figure 2

Figure 2

156x210mm (240 x 240 DPI)

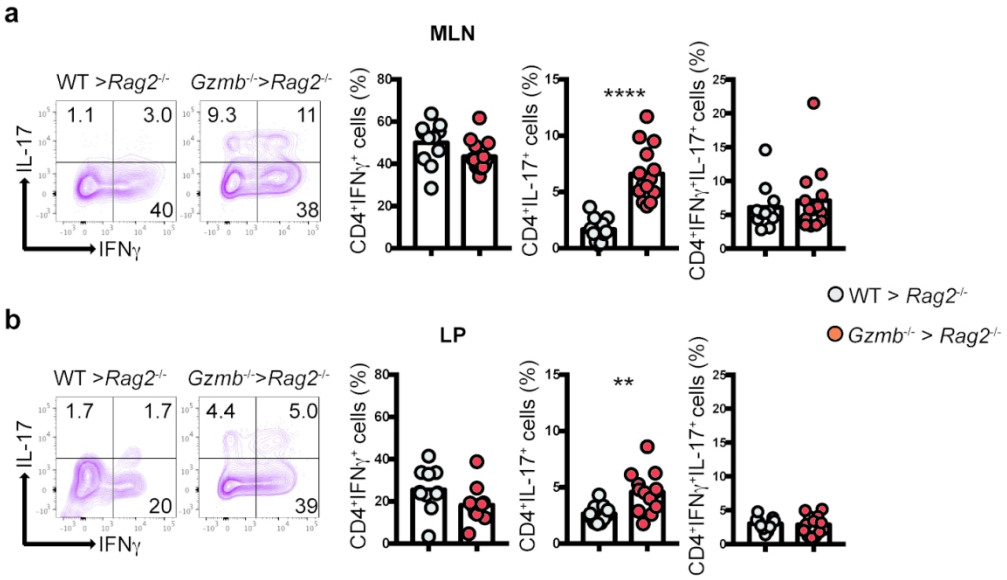

Figure 3

Figure 3

149x117mm (240 x 240 DPI)

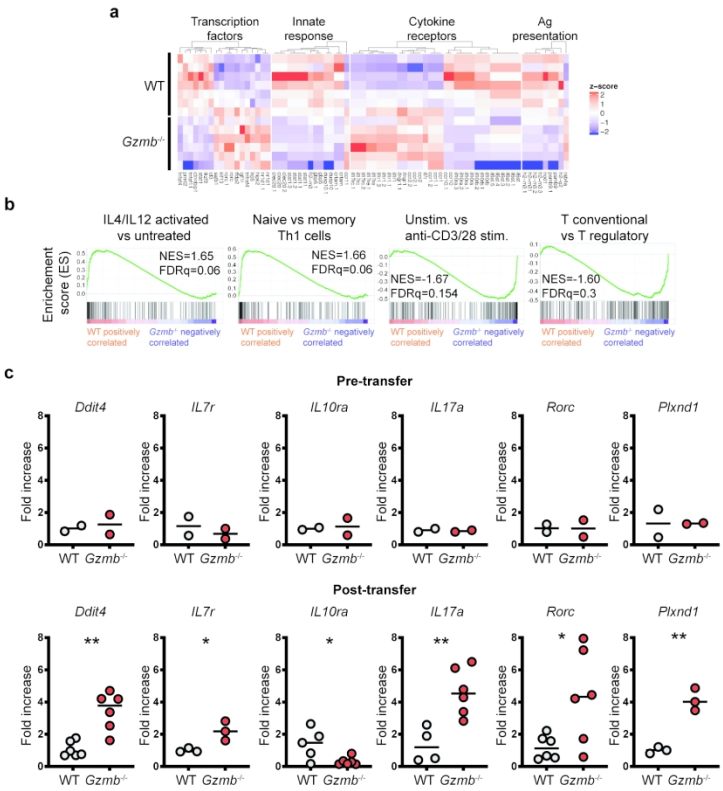

Figure 4

Figure 4

185x283mm (240 x 240 DPI)

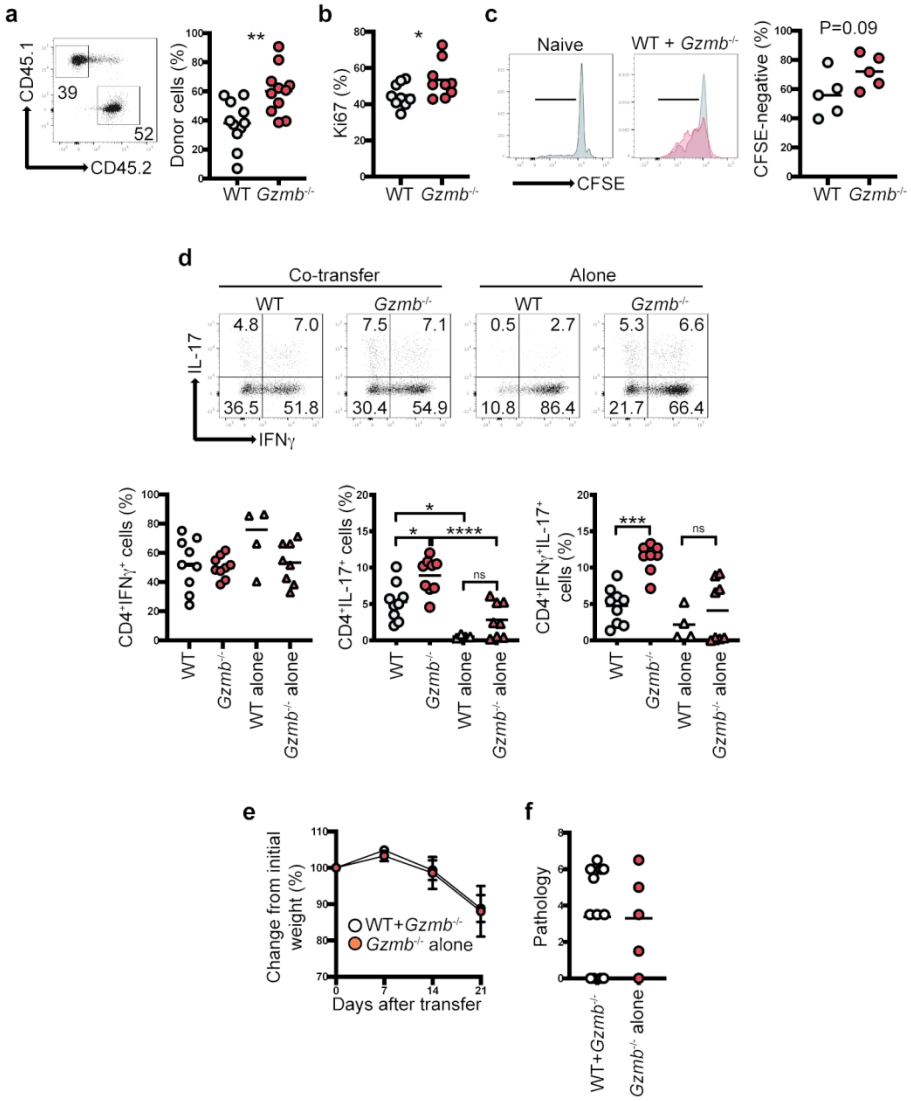

Figure 5

Figure 5

157x209mm (240 x 240 DPI)

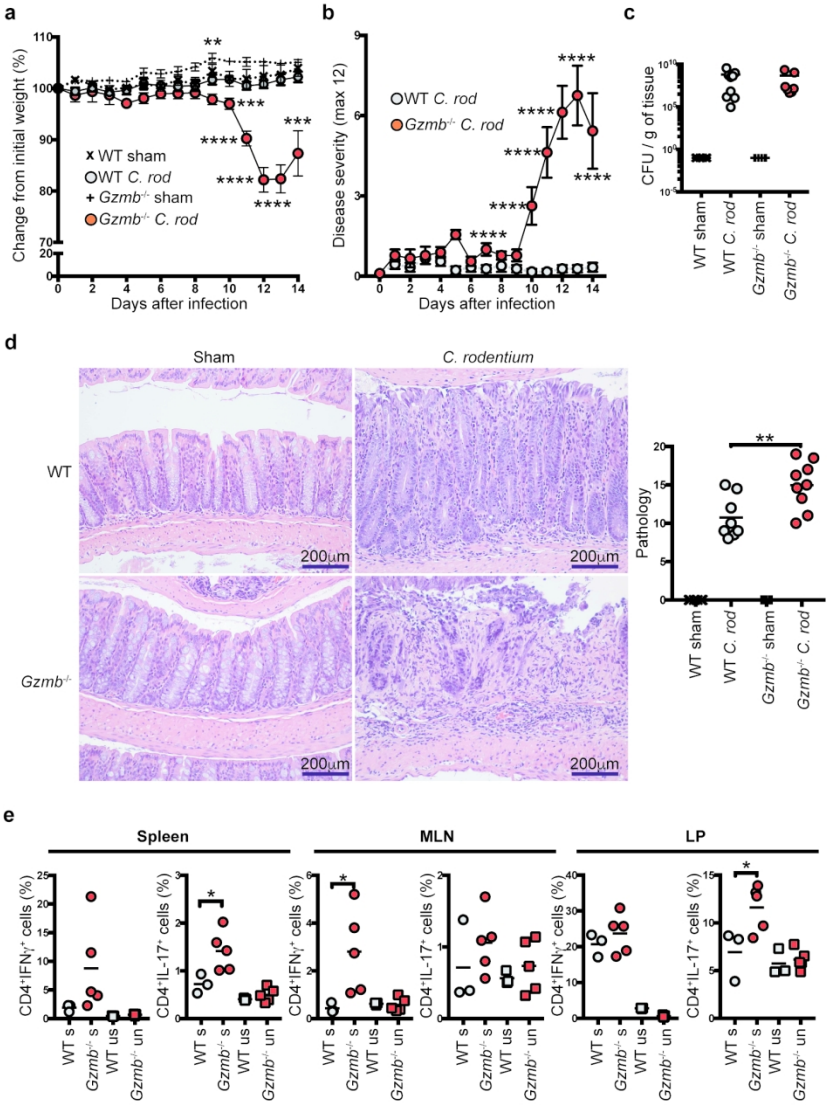

Figure 6

Figure 6

164x238mm (240 x 240 DPI)

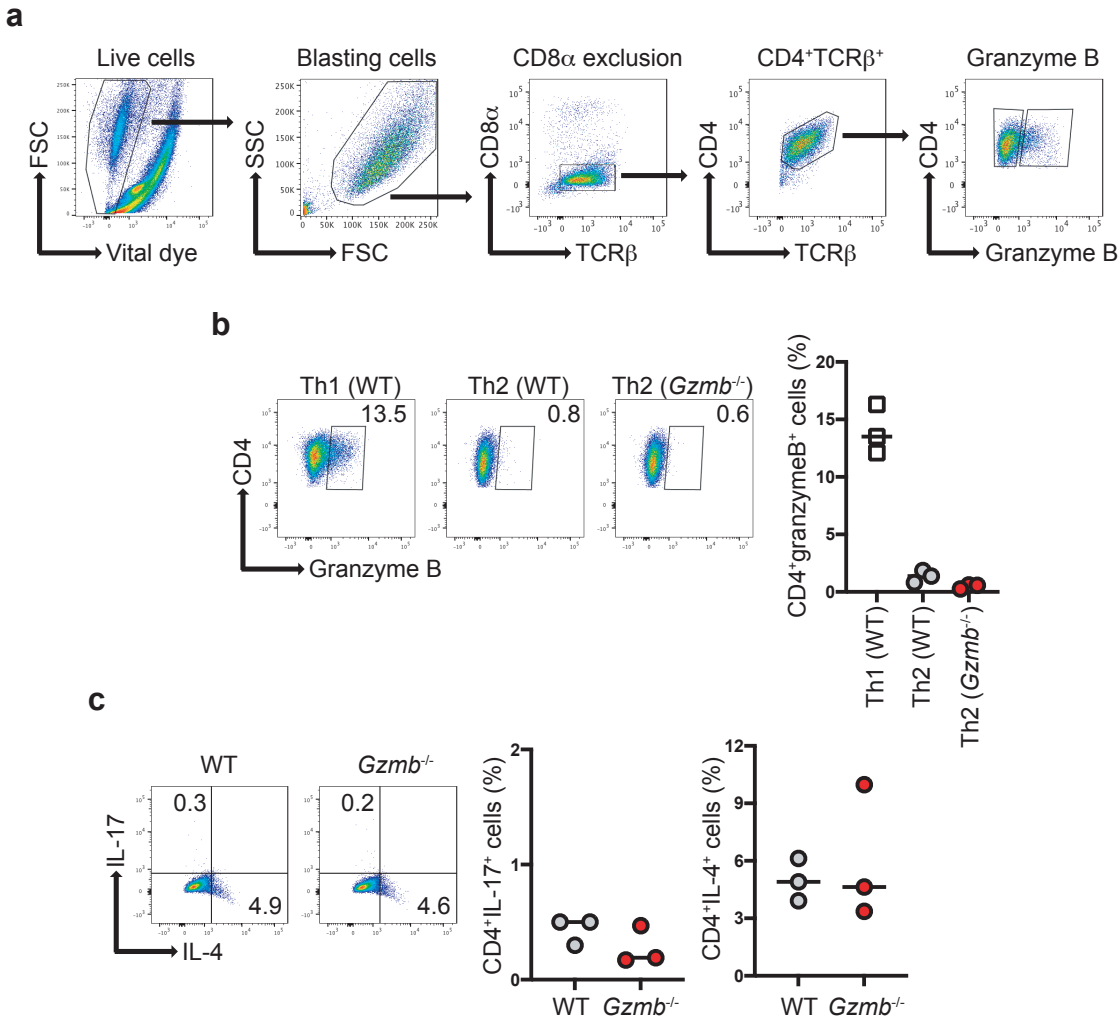

Supplemental Figure 1

Supplemental Figure 1. (a) Gating strategy for Figure 1. Plots are from representative WT $CD4^+$ T cells cultured in Th0 conditions. Cells from *Gzmb*$^{-/-}$ mice presented similar gating profiles (not shown). (b) Granzyme B expression in differentiated Th1 and Th2 cells from the indicated mice; left, representative dot plots; right, summary. n=3. (c) IL-17 and IL-4 expression in Th2 differentiated cells from the indicated mice; left, representative dot plots; right, summary. n=3.

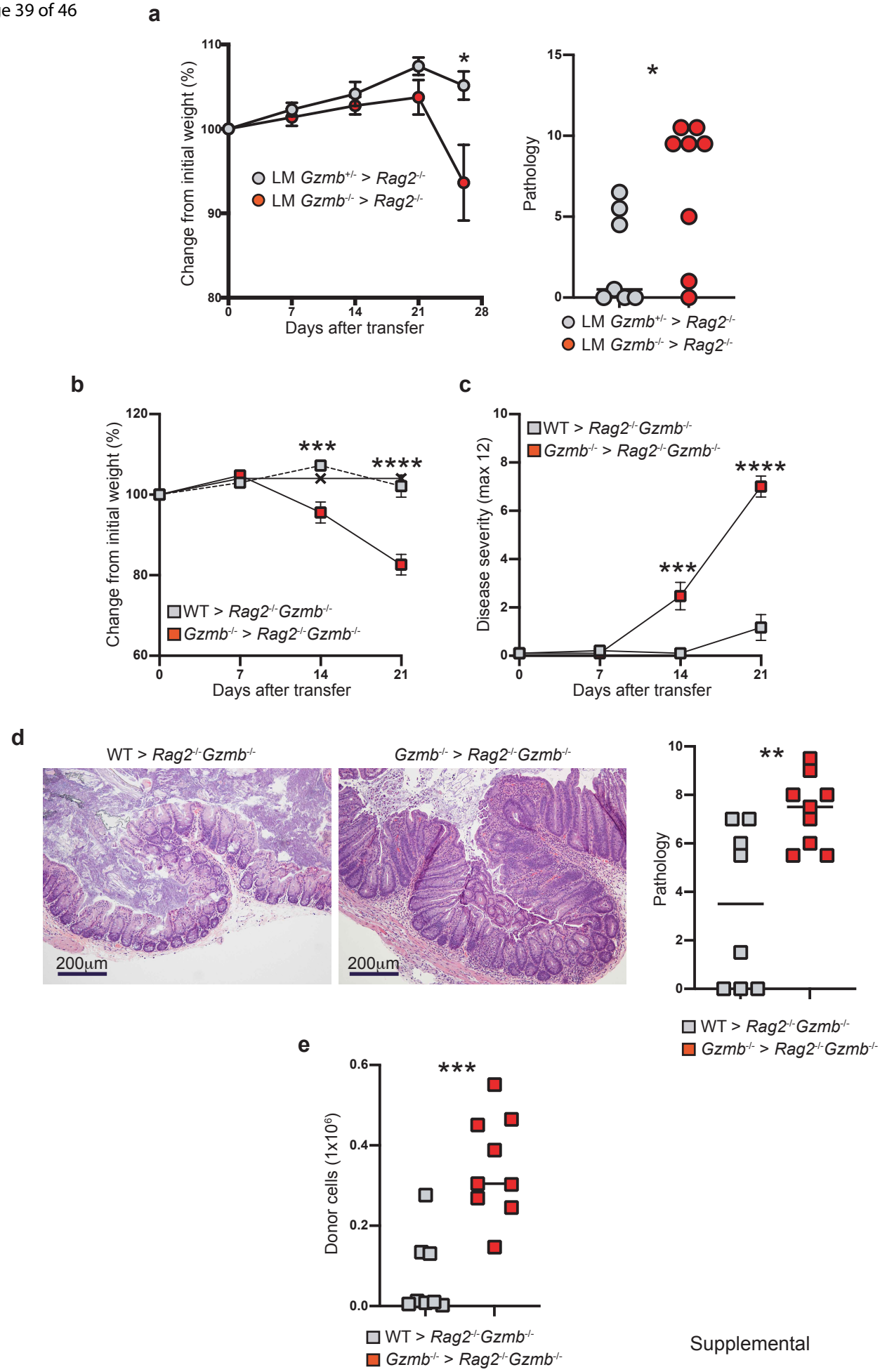

Supplemental

Figure 2

Supplemental Figure 2. *In vivo* activated granzyme B-deficient $CD4^+$ T cells display increased pathogenicity. (a) $1x10^5$ $CD4^+CD45RB^{hi}$ T cells from *Gzmb*$^{+/-}$ or *Gzmb*$^{-/-}$ littermate donor mice were transferred into *Rag2*$^{-/-}$ recipient mice and their weights monitored weekly (left), and colon pathology scored (right). (b-e) $1x10^5$ $CD4^+CD45RB^{hi}$ T cells from WT or *Gzmb*$^{-/-}$ donor mice were adoptively transferred into *Rag2*$^{-/-}$*Gzmb*$^{-/-}$ recipient mice; (b) mice were weighed weekly, and (c) monitored for signs of disease. Twenty-one days after transfer, (d) colon pathology was scored (left, representative micrographs; right, data summary), and (e) donor-cell reconstitution of the IEL compartment in the colon was determined. For (a), dotted lines represent untreated *Rag2*$^{-/-}$*Gzmb*$^{-/-}$ mice. Each dot represents an individual mouse. Data are representative of at least 3 independent experiments. n=8-9. *P<0.05; **P<0.01; ***P<0.001; ****P<0.0001; Student's t-test.

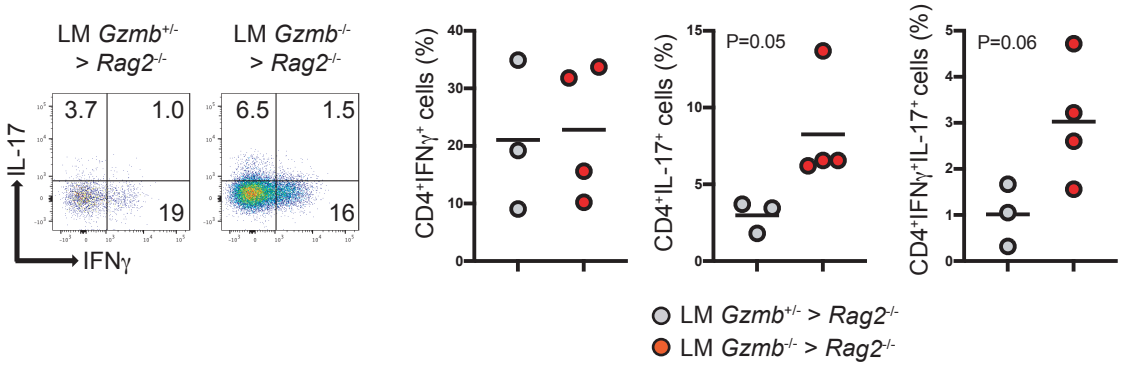

Supplemental

Figure 3

Supplemental Figure 3. Granzyme B-deficient $CD4^+$ T cells present skewed IL-17 differentiation *in vivo.* $1x10^5$ $CD4^+CD45RB^{hi}$ T cells from littermate *Gzmb*$^{+/-}$ or *Gzmb*$^{-/-}$ donor mice were adoptively transferred into *Rag2*$^{-/-}$ recipient mice. Three weeks after transfer, donor-derived cells were recovered from MLN and their IFNγ/IL-17 profile was determined by intracellular staining. Dot plots indicate a representative sample. Live, $TCR\beta^+CD4^+$ cells are displayed. Graphs represent the summary. n=3. Each dot indicates an individual mouse. Student's t-Test.

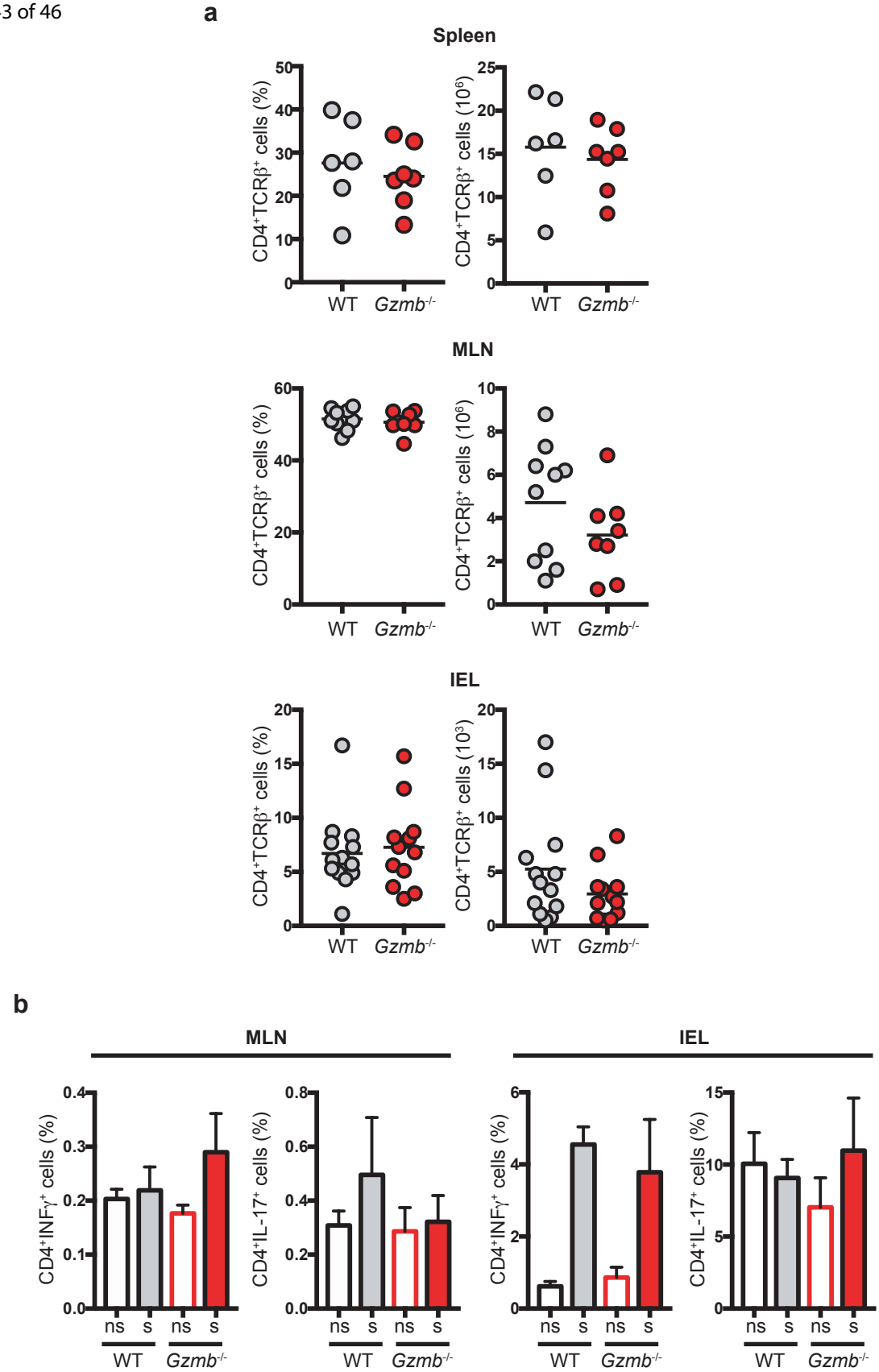

Supplemental Figure 4

Supplemental Figure 4. Naïve granzyme B-deficient mice display a normal $CD4^+$ T cell compartment. (a) $CD4^+$ T cell frequencies and cellularity from spleen, MLN, and IEL compartment were determined by flow cytometry. (b) *Ex vivo* single cytokine positive $CD4^+$ T cells derived from naïve WT and *Gzmb*$^{-/-}$ mice. Cells were non-stimulated (ns) or stimulated (s) for 4 h with PMA/ionomycin. Each dot represents an individual mouse. For (a), spleen and MLN, n=6-10; for IEL, n=12-13. For (b), n=6.

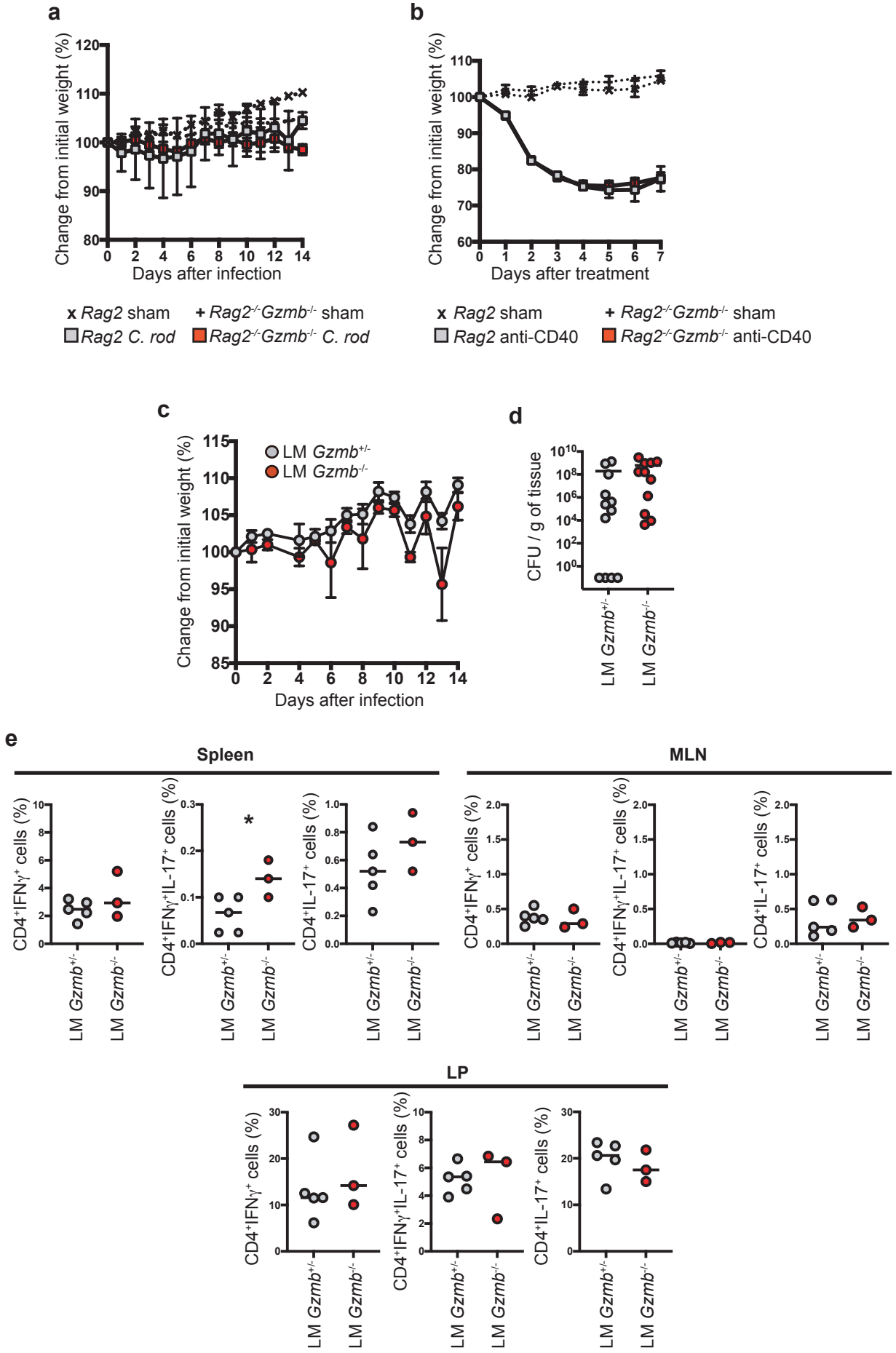

Supplemental Fig. 5

Supplemental Figure 5. (a) Absence of adaptive immune cells rescues granzyme B-deficient mice from severe disease. The indicated mice were orogastrically infected with *C. rodentium* ($5x10^8$ CFU/mouse) and monitored for weight change for 14 days. Data are representative of at least 2 independent experiments. n=3-4 for sham groups. n=5-7 for infected mice. (b) Granzyme B deficiency does not alter disease progression in the anti-CD40 model of colitis. The indicated mice were treated i.p. with 150 μg/mouse and weighed daily. Data are representative of at least 3 independent experiments. n=2 for sham groups. n=14 for treated group. (c-e) Littermate *Gzmb*$^{+/-}$ and *Gzmb*$^{-/-}$ mice were infected with *C. rodentium* ($5x10^8$ CF/mouse). (c) Animals were monitored daily for weight change. At 14 days post infection, (d) colon colonization and (e) IFNγ and IL-17 production were determined in the indicated organs. For (c and d), n=11-12; for (e), n=3-5. Student's t-Test. *P<0.05.